Circ J 2009; **73:** 39–47

d,l-Sotalol at Therapeutic Concentrations Facilitates the Occurrence of Long-Lasting Non-Stationary Reentry During Ventricular Fibrillation in Isolated Rabbit Hearts

Yu-Cheng Hsieh, MD; Tzyy-Leng Horng, PhD*; Shien-Fong Lin, PhD**; Tung-Chao Lin, MD; Chih-Tai Ting, MD, PhD; Tsu-Juey Wu, MD, PhD

Background The effects of *d,l*-sotalol at therapeutic concentrations (≤10 mg/L) on wavefront dynamics during ventricular fibrillation (VF) and electrophysiological heterogeneity remain unclear.

Methods and Results By using an optical mapping system, epicardial activation patterns of VF were studied in 6 Langendorff-perfused rabbit hearts at baseline, during 10 mg/L *d,l*-sotalol infusion, and after washout. In an additional 4 hearts, action potential duration (APD), conduction velocity, and wavelength (WL) restitutions were determined. During *d,l*-sotalol infusion, VF was terminated in 3 of the 6 hearts. Only 1 heart developed transient ventricular tachycardia (VT). *d,l*-Sotalol reduced the number of phase singularities (ie, wavebreak) during VF ($P<0.05$), and it also increased the occurrence frequency ($P<0.05$) and lifespan ($P<0.05$) of epicardial reentry during VF. These reentries were non-stationary in nature and did not anchor on anatomical structures. Restitution data showed that *d,l*-sotalol flattened APD restitution. Furthermore, APD dispersion and spatial heterogeneity of restitutions were not enhanced by *d,l*-sotalol.

Conclusions *d,l*-Sotalol at therapeutic concentrations decreased wavebreak and facilitated the occurrence of long-lasting, non-stationary reentry during VF. However, VT rarely occurred. The related mechanisms include: (1) flattening of APD restitution without enhancement of spatial heterogeneity of electrophysiological properties, causing wavefront organization, and (2) WL prolongation, preventing steady anchoring of reentry. (*Circ J* 2009; **73:** 39–47)

Key Words: *d,l*-sotalol; Reentry; Ventricular fibrillation

On the basis of the ESVEM trial, *d,l*-sotalol has been approved for the treatment of life-threatening ventricular tachycardia (VT) and ventricular fibrillation (VF)[1,2] It has been shown that *d,l*-sotalol reduces the complexity of epicardial activation patterns and prolonged wavelength (WL) during VF in isolated rabbit hearts.[3] Recently, Pak et al reported that *d,l*-sotalol at therapeutic doses (≤10 mg/L) effectively terminated VF/VT by flattening the action potential duration restitution (APDR) in isolated swine ventricles.[4] However, the effects of *d,l*-sotalol at therapeutic concentrations on the wavefront characteristics of VF and the genesis of electrophysiological heterogeneity (such as action potential duration (APD) dispersion and spatial heterogeneity of restitutions) are still not completely understood.

We previously demonstrated that 2 types of VF exist in the same isolated rabbit heart.[5] As APDR was flattened by low-dose methoxyverapamil (D600), multiple-wavelet type 1 VF was converted to VT. A further increase of D600 concentration converted VT to a slower (type 2) VF with a stationary or slow drifting mother rotor. During type 2 VF, an anatomical structure (the papillary muscle (PM)), always served as an anchoring site for the mother rotor.[6,7] We hypothesized that *d,l*-sotalol at therapeutic concentrations, with both its effects of APDR flattening and WL prolongation, would also convert a preexisting type 1 VF into a regular rhythm, finally leading to termination of the ventricular tachyarrhythmia. To test this hypothesis, an optical mapping system was used to record epicardial activation patterns during *d,l*-sotalol infusion in isolated rabbit hearts. The aims of this study were to determine (1) whether or not acute administration of *d,l*-sotalol can effectively convert a preexisting VF into VT before its termination, and (2) the wavefront characteristics of VF and the electrophysiological heterogeneity during *d,l*-sotalol infusion with therapeutic concentrations.

Methods

This research protocol was approved by the Institutional Animal Care and Use Committee of Taichung Veterans General Hospital and followed the guidelines of American

(Received June 5, 2008; revised manuscript received July 19, 2008; accepted August 5, 2008; released online November 13, 2008)

*Cardiovascular Center, Taichung Veterans General Hospital, Taichung and Department of Internal Medicine, Faculty of Medicine, Institute of Clinical Medicine, Cardiovascular Research Center, National Yang-Ming University School of Medicine, Taipei, *Department of Applied Mathematics, Feng-Chia University, Taichung, Taiwan and **Krannert Institute of Cardiology and the Division of Cardiology, Department of Medicine, Indiana University School of Medicine, Indianapolis, IN, USA*

Mailing address: Tsu-Juey Wu, MD, PhD, Cardiovascular Center, Taichung Veterans General Hospital, 160, Section 3, Chung-Kang Road, Taichung, Taiwan. E-mail: tjwu@vghtc.vghtc.gov.tw

Table 1 Effects of *d,l*-Sotalol on the APD, CT^{-1} and WL

	S1 PCL, ms										
	500	*400*	*300*	*250*	*200*	*180*	*160*	*150*	*140*	*130*	*120*	*110*
APD_{70} (ms)												
Baseline	*162±18*	*154±15*	*147±11*	*140±13*	*120±3*	*103±14*	*98±13*	*93±12*	*88±13*	*79±10*	*78±13*	*70±11*
5 mg/L d,l-sotalol	*191±12†*	*185±14†*	*164±10†*	*149±12†*	*130±8*	*118±6*	*114±20*	*103±11*	*95±14*	*101±6*	*93±0**	*80±0**
10 mg/L d,l-sotalol	*223±15††*	*213±15††*	*197±12††*	*182±17†*	*139±10*	*133±5***	*126±3***	*112±1***	*105±4***	*102±5***	*NA*	*NA*
CT^{-1} (cm/s)												
Baseline	*66±10*	*66±11*	*64±12*	*63±12*	*61±12*	*61±10*	*61±10*	*60±10*	*57±9*	*57±9*	*56±9*	*53±9*
5 mg/L d,l-sotalol	*69±6*	*69±7*	*68±7*	*68±7*	*67±9*	*65±7*	*64±7*	*63±7*	*62±7*	*65±5*	*68±0**	*68±0**
10 mg/L d,l-sotalol	*68±9*	*67±10*	*67±10*	*66±11*	*70±11*	*72±4***	*72±4***	*72±4***	*69±3***	*68±3***	*NA*	*NA*
WL (cm)												
Baseline	*10.6±0.2*	*10.0±0.2*	*9.7±2.2*	*8.7±1.6*	*7.4±1.0*	*6.4±1.5*	*6.0±1.1*	*5.6±1.5*	*5.1±1.2*	*4.5±1.1*	*4.4±1.2*	*3.7±1.0*
5 mg/L d,l-sotalol	*13.5±1.5†*	*12.7±1.6*	*11.1±1.1*	*10.0±1.2*	*8.7±1.2*	*7.8±1.0*	*7.3±1.8*	*6.5±1.3*	*6.0±1.3*	*6.5±0.6†*	*6.4±0**	*5.5±0**
10 mg/L d,l-sotalol	*15.0±1.0††*	*14.2±0.9††*	*13.2±1.6††*	*11.8±0.8†*	*9.8±1.8†*	*9.6±0.2***	*9.1±0.6***	*8.2±0.5***	*7.4±0.5***	*7.1±0.4***	*NA*	*NA*

**Data from heart #3 in protocol II without statistical comparison.*
***Data from hearts #3 and #4 in protocol II without statistical comparison.*
†P<0.05, ††P<0.01, by paired t-test when compared with baseline.
APD, action potential duration; CT^{-1}, inverse of conduction time; WL, wavelength; PCL, pacing cycle length; NA, data not available.

Heart Association.

Langendorff Preparation and Pseudo-ECG Recordings

The hearts of 10 New Zealand White rabbits (2.7–4.1 kg) were excised under general anesthesia. The ascending aorta was immediately cannulated and perfused with 36.5°C Tyrode's solution with the following composition (in mmol/L): 125 NaCl, 4.5 KCl, 0.5 $MgCl_2$, 24 $NaHCO_3$, 1.8 NaH_2PO_4, 1.8 $CaCl_2$, 5.5 glucose, and albumin (40 mg/L); it was then equilibrated with 95% O_2 and 5% CO_2 to maintain a pH of 7.4[8] Coronary perfusion pressure was then regulated with a flow rate of 25–30 ml/min[5,6] Next, the hearts were perfused and superfused in a thermostatized tissue bath made of transparent glass. The bath temperature remained at a constant value within the range of 36–37°C during the experiment. A pseudo-ECG was obtained with widely spaced bipoles, 1 at the apex of the left ventricle (LV) and the other at the high lateral wall of the right ventricle (RV). The signals were filtered from 0.05 to 100 Hz, and were digitized by an AxoScope with a sampling rate of 1 kHz[5,6,8,9] The pseudo-ECG was used to determine the rhythm of the ventricles.

Optical Mapping

A single-camera optical mapping system was used and has been described previously[5,6] The hearts were stained with di-4-ANEPPS (Molecular Probes, Eugene, OR, USA), then excited with quasi-monochromatic light (500±40 nm) from a 250-W tungsten–halogen lamp. Fluorescent and scattered lightwaves from the heart were collected by an image-intensified charge-coupled device camera (Dalsa Inc, Waterloo, Ontario, Canada). The optical signals were gathered at 3.75-ms sampling intervals, acquired from 100×100 sites simultaneously over a 40×40-mm^2 area. For each time window of recording, the optical data were acquired continuously for 2.25 s (ie, 600 frames). Phase mapping was performed to evaluate the wavefront characteristics and the location and evolution of phase singularities (PSs) during VF[10] In a typical time-embedded phase portrait, the upstroke of the action potential corresponds to a phase ranging from $-3/4\ \pi$ to $-1/4\ \pi$, roughly the light-blue color (between dark-blue and green) using color representation[5,6,8,9] Optically recorded voltage signals were spatiotemporally filtered to reduce noise[11] The mapped area included parts of the RV and LV anterior walls.

Study Protocols

Protocol I: Effects of d,l-Sotalol at Therapeutic Concentrations on the Wavefront Characteristics and Inducibility of VF (n=6) A hook bipolar electrode was inserted into the RV outflow tract for pacing[5,6,8,9] We used burst pacing (cycle length (CL) 75–100 ms; current 5–10 mA) to induce baseline VF. Baseline VF was defined as stable VF that persisted for 5 min after pacing induction[5,6,8,9] Three sets of optical mapping data and corresponding pseudo-ECG recordings were obtained during baseline VF. *d,l*-Sotalol at a concentration of 10 mg/L was then infused for 30 min to observe changes in ventricular rhythm, such as VF/VT transition and VF termination. Optical and corresponding pseudo-ECG recordings were obtained every 3–5 min, including 5, 15, and 25 min of *d,l*-sotalol infusion. If the VF episode persisted without termination for 30 min, it was defined as no termination by *d,l*-sotalol. When the VF episode was successfully converted to spontaneous (sinus/idioventricular) rhythm, 3 burst pacing attempts were

immediately performed to determine VF inducibility. VF inducibility was defined as the ratio of the successful VF induction instances to the number of burst pacing attempts.[4,12] Successful VF induction was defined as VF persisting for at least 3 min after cessation of burst pacing. *d,l*-Sotalol was then washed out with drug-free Tyrode's solution for 30 min and VF inducibility was again determined.

Protocol II: Restitution Curves (n=4) To estimate the conduction velocity (CV), the inverse of conduction time (CT^{-1}, cm/s) between 2 epicardial points was measured.[5] We used the S_1 pacing method to determine APD and CT^{-1} restitutions at baseline and at the end of the 30-min infusion of different *d,l*-sotalol concentrations (5 and 10 mg/L) sequentially. APD and CT^{-1} restitutions were determined using 12 different S_1 pacing CLs (500, 400, 300, 250, 200, 180, 160, 150, 140, 130, 120, and 110 ms) in all 4 hearts studied.[5] To minimize motion artifacts, an adjustable glass wall was used to compress and restrain the heart during pacing.

Data Analysis

Fast Fourier Transform (FFT) Analysis FFTs of the pseudo-ECGs (4s in duration) were used to determine the dominant frequency (DF) at 5 different time points of VF in protocol I: (1) baseline VF (no *d,l*-sotalol), (2) VF after 5-min *d,l*-sotalol infusion, (3) VF after 15-min *d,l*-sotalol infusion, (4) VF after 25-min *d,l*-sotalol infusion, and (5) VF after washout (ie, the re-induced VF after 30-min washout).

Epicardial Activation Patterns During VF We also evaluated the wavefront characteristics of VF at the same 5 time points, analyzing 2–3 time windows of optical recording in each heart studied. Each time window of optical recording contained 600 phase maps (ie, 600 frames), which were gathered every 3.75 ms for a total of 2.25 s.

To characterize the complexity of the wavefront dynamics during VF, the number of PSs in each phase map was counted manually throughout the 600 frames in each optical recording to obtain the average number of PSs.[13–15] PSs were defined as sites with an ambiguous phase surrounded by pixels exhibiting a continuous phase progression from $-\pi$ to $+\pi$.[13–15]

To evaluate the characteristics of epicardial reentry, such as life span (ie, rotations) and trajectory of core (ie, stationary or non-stationary), during different time points of VF, optical mapping data were displayed frame-by-frame.[8] In addition, the percentage of recording time containing at least 1 epicardial reentry was also determined. The core was defined as the area encircled by the reentrant wavefront. Epicardial reentry was considered stationary when the tip of the reentrant wavefront, which circulated around the core, followed a closed circular or elliptical trajectory and the periodicity was preserved everywhere outside the core.[16] Otherwise, it was considered non-stationary. The location of the core was determined by tracing the trajectory of the tips of the wave propagation.[16] On the phase maps, the tip of the reentrant wavefront was shown as a PS point.

Construction of APD and CT^{-1} Restitution Curves by S_1 Pacing Method The details of constructing the APD and CT^{-1} restitution curves have been reported elsewhere.[5] Briefly, 1 pixel at the center of the 4 quadrants in the mapped area is used to determine the APD_{70} (sites a to d, see Fig 1C in Reference 5).[5] APD_{70} was the APD measured at 70% repolarization, and diastolic interval (DI) was the interval between the previous APD_{70} point and the next initiation point of the action potential.[5] An APDR curve was then constructed by plotting the means of APD_{70} (ms) obtained from the 4 sites against different S_1 pacing CLs. Because CT^{-1} at the ventricular surface was not homogeneous, we used the mean of CT^{-1} along 4 evenly distributed epicardial lines to construct CT^{-1} restitution (lines 1–4, see Fig 1B in Reference 5).[5] CT^{-1} restitution of each heart was constructed by plotting the means of CT^{-1} along the 4 epicardial lines against different S_1 pacing CLs. By using the formula $APD_{70} \times CT^{-1} = WL$ (cm), WL restitutions were constructed.

Determination of Maximum Slope of APDR Curve by S_1 Pacing Method To determine the maximum slope of the

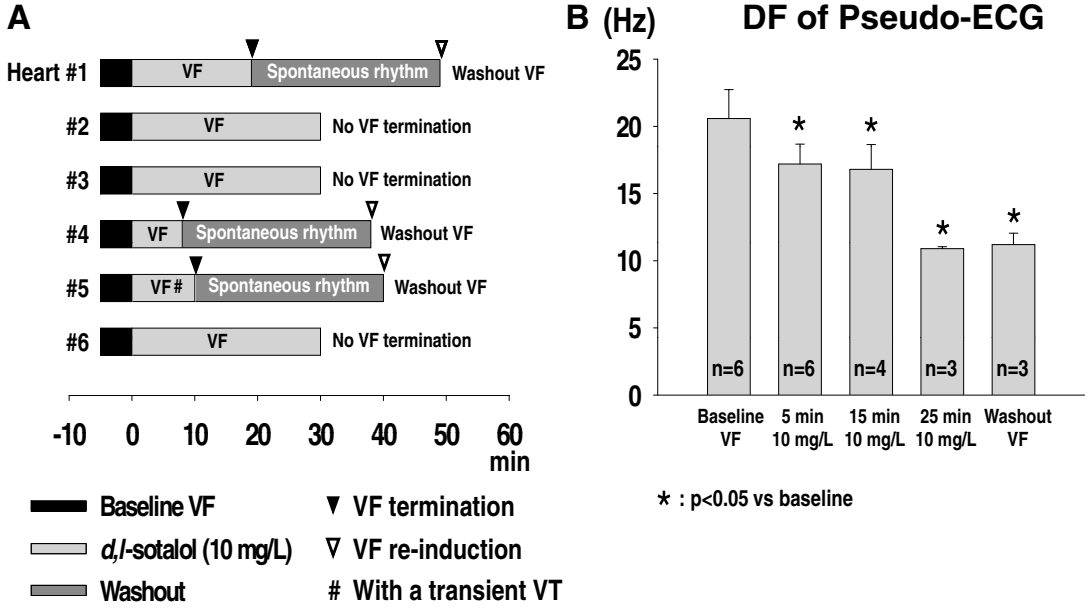

Fig 1. (**A**) Effect of 10 mg/L *d,l*-sotalol on VF/VT transition and VF termination with respect to elapsed time in all 6 hearts in protocol I. (**B**) Effect of 10 mg/L *d,l*-sotalol on the mean DF of pseudo-ECG in protocol I. n = number of hearts studied. DF, dominant frequency; VF, ventricular fibrillation; VT, ventricular tachycardia.

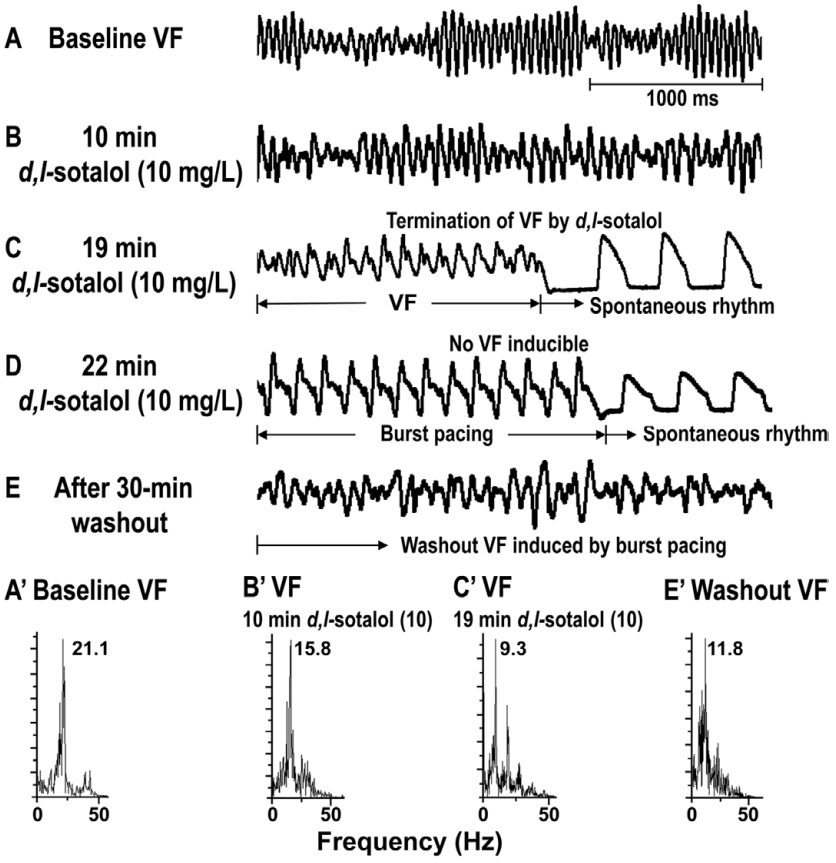

Fig 2. Example of the effects of *d,l*-sotalol on pseudo-ECG and DF in VF (data from heart #1). (**A**–**E**) Pseudo-ECG of VF at baseline (**A**), 10 mg/L *d,l*-sotalol infusion (**B**), VF termination (**C**), VF inducibility test (**D**), and washout period (**E**). (**A'**–**E'**) DF for corresponding pseudo-ECG tracings in **A**–**E**. See text for details.

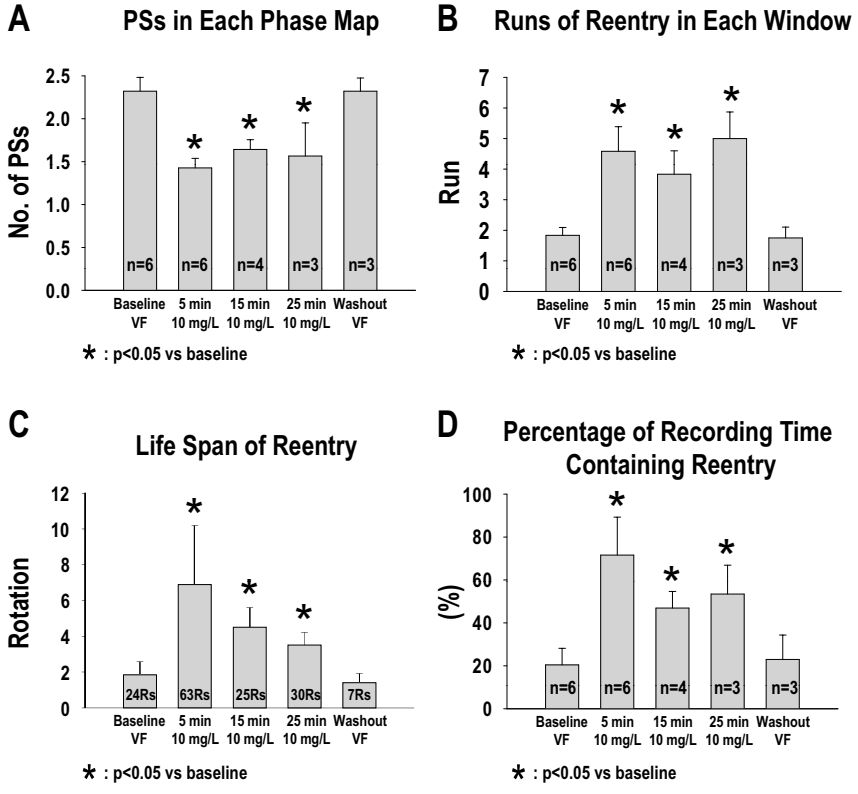

Fig 3. Effects of *d,l*-sotalol on wavefront characteristics during different time points of VF in protocol I. (**A**) Average number of phase singularities (PSs) in each phase map. (**B**) Runs of epicardial reentry observed in each recording time window. (**C**) Life span (in rotations) of epicardial reentry. (**D**) Percentage of recording time containing at least 1 epicardial reentry. n = number of hearts studied. See text for details.

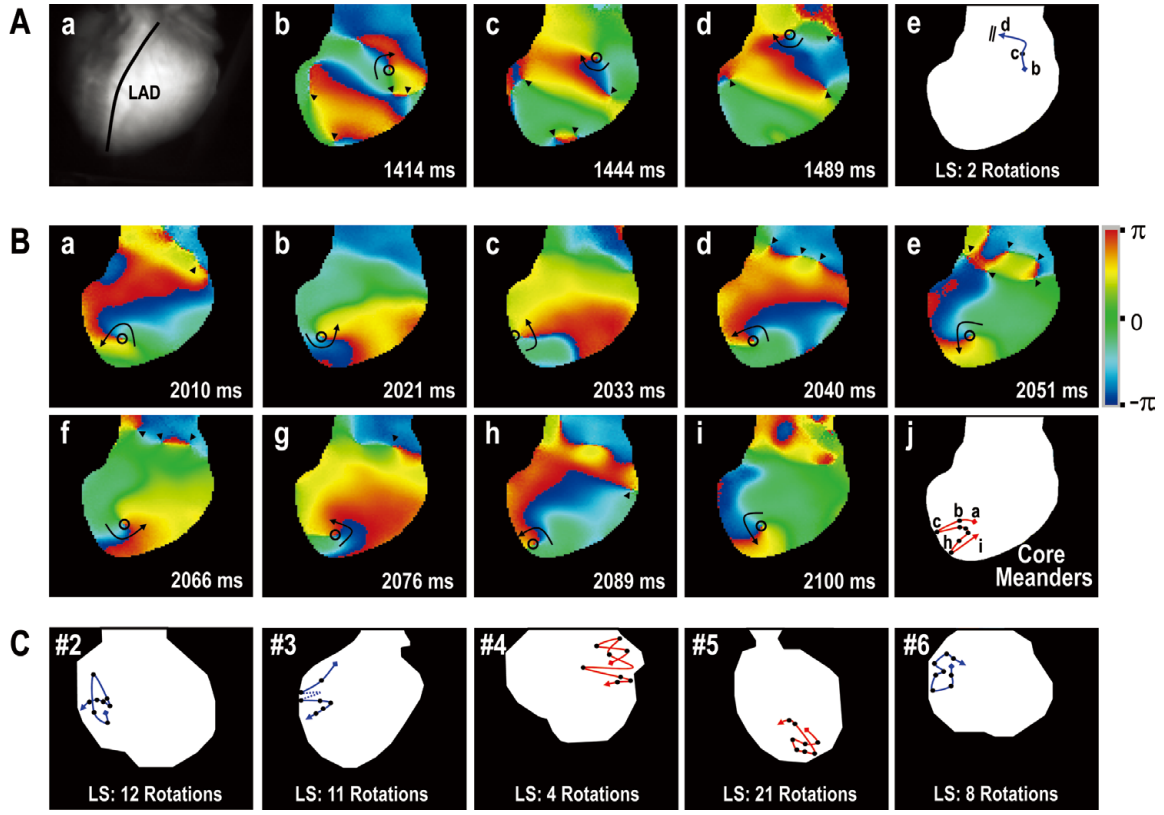

Fig 4. (**A**) Example of short-lived reentry during VF before administration of *d,l*-sotalol (data from heart #1). In **Ab**–**Ad**, black circles indicate the location of the core of reentry. Arrowheads indicate PSs. (**B**, **C**) Examples of non-stationary reentry during VF with 10 mg/L *d,l*-sotalol infusion. (**B**) Drifting reentry recorded 7 min after the onset of *d,l*-sotalol infusion (data from heart #1). This run of reentry had a life span of 36 rotations, lasting from 578 to 2,250 ms. (**Ba**–**Bi**) Phase maps showing that this reentry first drifted to the border of the mapped area (**Bc**), again into the right ventricle (**Bd**), and finally to the interventricular septum (**Be**–**Bi**). Trajectory of the core, demonstrating a meandering nature (**Bj**). (**C**) Another 5 examples of the trajectory of the core of non-stationary reentry (1 each from hearts #2–6, respectively). Red colored trajectory indicates counterclockwise rotation. Blue colored trajectory indicates clockwise rotation. Aa, mapped area; Ae, trajectory of the core; LAD, left anterior descending coronary artery; LS, life span of reentry; PS, phase singularities; VF, ventricular fibrillation.

APDR in each heart, APDR curves of the 4 sampling pixels (a to d) were re-plotted using APD_{70} against the preceding DI. The maximum slope of the APDR in these 4 sites was then calculated by first-order exponential fitting with ORIGIN software (Microcal)[5]. The maximum slope of the APDR in each heart was the mean of the maximum APDR slopes obtained from these 4 sites at baseline and with different *d,l*-sotalol concentrations.

Determination of APD Dispersion APD dispersion (ms) was defined as the difference between the maximum and minimum APD_{70} obtained from every pixel distributed over the mapped area during S_1 pacing.

Statistical Analysis

Data are presented as mean±SD. Paired or unpaired t-tests were used to compare the results of FFT analysis and the characteristics of epicardial reentry at different time points of VF in protocol I. Paired t-tests were used to evaluate the effects of *d,l*-sotalol on the APD, CT^{-1}, and WL in protocol II (**Table 1**). We also used ANOVA with repeated measurements to compare the results of the maximum slope of the APDR, APD dispersion, and spatial heterogeneity of restitutions at baseline and *d,l*-sotalol (5, 10 mg/L) infusion[5]. A probability value ≤0.05 was considered significant.

Results

Protocol I

VF/VT Transition and VF Termination During d,l-Sotalol Infusion Baseline VF was successfully induced by burst pacing in all 6 hearts studied. With 10 mg/L *d,l*-sotalol infusion, VF was eventually terminated in 3 (#1, #4, and #5). The mean elapsed time for VF termination was 12.3±5.9 min (ranging from 8 to 19 min); 2 of the 3 hearts showed abrupt VF termination without a transition to VT. Only heart #5 showed a transient VT (3 min in duration) 1 min after the initiation of *d,l*-sotalol infusion, which was followed by a 6-min VF that subsequently terminated. The VF inducibility was 0% in all 3 hearts immediately after VF termination; however, it increased to 100% in each heart after the 30-min washout. **Fig 1A** summarizes the effects of 10 mg/L *d,l*-sotalol on VF/VT transition and VF termination with respect to elapsed time. FFT analyses of the pseudo-ECG showed that *d,l*-sotalol significantly reduced mean DF even during the washout period (20.6±2.1, 17.2±1.5*, 16.8±1.8*, 10.9±0.2*, and 11.2±0.9* Hz for baseline, 5-min, 15-min, 25-min *d,l*-sotalol infusion, and washout, respectively; *P<0.05 when compared with baseline) (**Fig 1B**). **Fig 2** is a clear example, showing the effects of *d,l*-sotalol on the pseudo-ECG and DF in VF. With the infusion of 10 mg/L

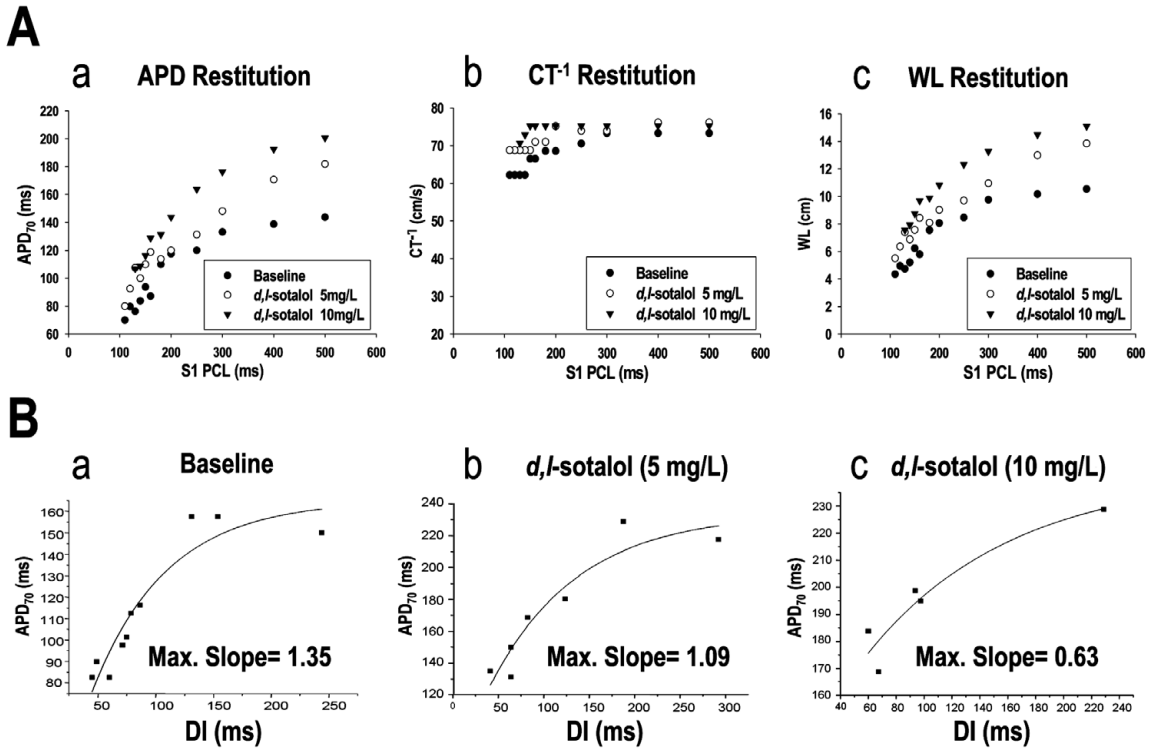

Fig 5. (**A**) Effects of *d,l*-sotalol on APD, CT^{-1} and WL restitutions. Data obtained from heart #3 in protocol II. (**B**) Effects of *d,l*-sotalol on the maximum slope of APDR. Data obtained from site b of heart #4 in protocol II. See text for details. APD, action potential duration; APDR, action potential duration restitution; CT^{-1}, inverse of conduction time; WL, wavelength.

d,l-sotalol, the DF of the pseudo-ECG progressively decreased from 21.1 (baseline, **Figs 2A**, **A'**) to 15.8 Hz (10-min *d,l*-sotalol infusion, **Figs 2B**, **B'**). At 19 min after the onset of *d,l*-sotalol infusion, this VF episode abruptly terminated with a DF of 9.3 Hz (**Figs 2C**, **C'**). Burst pacing immediately after VF termination failed to induce any VF episode (**Fig 2D**). After washout, burst pacing again easily induced VF with a corresponding DF of 11.8 Hz (**Figs 2E**, **E'**).

Epicardial Activation Patterns During VF We analyzed 47 time windows of optical recording obtained at 5 different time points of VF: (1) baseline VF, 13 windows from 6 hearts; (2) VF after 5-min *d,l*-sotalol infusion, 14 windows from 6 hearts; (3) VF after 15-min *d,l*-sotalol infusion, 8 windows from 4 hearts; (4) VF after 25-min *d,l*-sotalol infusion, 6 windows from 3 hearts; and (5) VF after washout, 6 windows from 3 hearts. In these windows, a total of 149 runs of epicardial reentry (24, 63, 25, 30, and 7 runs for baseline, 5-min, 15-min, 25-min *d,l*-sotalol infusion, and washout, respectively) were identified and studied.

Number of PSs In the baseline VF, optical mapping showed multiple wandering wavelets and short-lived reentry. The average number of PSs in each phase map was 2.3±0.2. After *d,l*-sotalol infusion, the epicardial activation pattern became more organized with the occurrence of long-lasting non-stationary reentry. The average number of PSs in each phase map significantly decreased during *d,l*-sotalol infusion (1.4±0.1*, 1.6±0.1*, and 1.6±0.3* for 5-min, 15-min, and 25-min *d,l*-sotalol infusion, respectively; *P<0.05 when compared with baseline). After washout, optical mapping again showed multiple wandering and short-lived wavelets with an average PS of 2.3±0.1 (P=NS) (**Fig 3A**).

Occurrence of Long-Lasting Non-Stationary Reentry Compared with baseline (1.8±0.3 runs/time window), infusion of *d,l*-sotalol significantly increased the occurrence of epicardial reentry in each time window of optical recording (4.6±0.8*, 3.8±0.8*, and 5.0±0.9* runs/time window for 5-min, 15-min, and 25-min *d,l*-sotalol infusion, respectively; *P<0.05 when compared with baseline). During the washout period, the frequency of epicardial reentry returned to the baseline level (1.8±0.4 runs/time window, P=NS) (**Fig 3B**).

The life span (rotation) of each of these reentries was also significantly increased by *d,l*-sotalol (1.8±0.7, 6.9±3.3*, 4.5±1.1*, 3.5±0.7*, and 1.4±0.5 rotations for baseline, 5-min, 15-min, 25-min *d,l*-sotalol infusion, and washout, respectively; *P<0.05 when compared with baseline) (**Fig 3C**). Similarly, the percentage of recording time containing at least 1 reentry was significantly higher during *d,l*-sotalol infusion (20±8%, 72±18%*, 47±8%*, 53±13%* for baseline, 5-min, 15-min, and 25-min *d,l*-sotalol infusion, respectively; *P<0.05 when compared with baseline). After washout, this percentage again returned to the baseline level (23±11%, P=NS) (**Fig 3D**).

With *d,l*-sotalol infusion, the reentries were non-stationary in nature. They always drifted in and out of the mapped area. **Figs 4B** and **C** show typical examples of organized reentry with a drifting core (1 from each heart in protocol I).

Protocol II

Effects of d,l-Sotalol on APD, CT^{-1}, and WL Restitutions The Effects of *d,l*-sotalol on APD, CT^{-1}, and WL restitutions in the 4 hearts studied were similar and are summarized in **Table 1**. *d,l*-Sotalol progressively lengthened the APD_{70} with increasing concentration throughout all pacing CLs. However, there was no significant effect of *d,l*-sotalol on the

CV (estimated by CT^{-1}) with increasing concentration in any pacing CL. Therefore, the infusion of *d,l*-sotalol led to the prolongation of WL, especially at 10 mg/L (**Table 1**). **Fig 5** shows the effects of 5 and 10 mg/L *d,l*-sotalol on APD, CT^{-1}, and WL restitutions. Increasing the *d,l*-sotalol concentration from 5 to 10 mg/L progressively prolonged APD_{70}, shifting the APDR curve upwards (**Fig 5Aa**); however, the CT^{-1} restitution curve remained flat (**Fig 5Ab**). The WL restitution curve, therefore, subsequently shifted upwards as a result of the prolongation of APD with increasing concentration of *d,l*-sotalol (**Fig 5Ac**).

Using the S_1 pacing method, the maximum slope of the APDR decreased progressively with increasing *d,l*-sotalol concentration (1.36±0.26, 1.03±0.06, and 0.90±0.16 for baseline, 5, and 10 mg/L *d,l*-sotalol infusion, respectively; P=0.015). **Figs 5Ba–c** shows an example.

Effects of d,l-Sotalol on APD Dispersion and Spatial Heterogeneity of Restitutions

APD Dispersion In all 4 hearts studied, APD_{70} prolonged progressively with increasing *d,l*-sotalol concentration; however, the *d,l*-sotalol had no significant effect on the spatial dispersion of APD_{70}. APD_{70} dispersion at an S_1 pacing CL of 300 ms was 52±6, 56±11, and 55±8 ms for baseline, 5, and 10 mg/L of *d,l*-sotalol infusion, respectively (P=0.735). Similarly, APD_{70} dispersion at an S_1 pacing CL of 250 ms was 64±10, 59±6, and 61±5 ms for baseline, 5, and 10 mg/L of *d,l*-sotalol infusion, respectively (P=0.666).

APD Restitution At baseline, the maximum slope of the APDR was similar among the 4 recording sites (site a, 1.11±0.49; b, 1.52±0.72; c, 1.50±0.28; d, 1.32±0.15; P=0.592). This heterogeneity remained insignificant with 5 mg/L (site a, 1.15±0.04; b, 1.25±0.45; c, 0.81±0.45; d, 0.93±0.18; P=0.277) and with 10 mg/L (site a, 0.90±0.52; b, 0.91±0.22; c, 0.67±0.14; d, 1.10±0.25; P=0.341) *d,l*-sotalol infusion.

CT^{-1} Restitution "Maximum CT^{-1} reduction" was used to estimate the heterogeneity of CT^{-1} restitution (cm/s)[5]. It was defined as the difference in CT^{-1} at the longest and the shortest S_1 pacing CLs (see figure 6B in reference 5)[5]. There was no significant difference in the maximum CT^{-1} reduction along the 4 different lines at baseline (line 1, 17±8; line 2, 10±7; line 3, 8±4; line 4, 7±3 cm/s; P=0.101). Heterogeneity remained insignificant with 5 mg/L (line 1, 13±6; line 2, 8±6; line 3, 8±2; line 4, 8±6 cm/s; P=0.466) or 10 mg/L (line 1, 4±5; line 2, 3±3; line 3, 5±4; line 4, 10±6 cm/s; P=0.164) *d,l*-sotalol infusion.

Discussion

This study has the following major findings. (1) *d,l*-Sotalol at therapeutic concentrations flattened the APDR, decreased the number of PS (ie, wavebreak), and facilitated the occurrence of long-lasting non-stationary reentry, therefore reducing the complexity of VF activation; however, VT rarely occurred. (2) *d,l*-Sotalol prolonged the APD_{70} and WL without enhancing APD dispersion or the spatial heterogeneity of restitutions.

Complexity of VF Activation Reduced by d,l-Sotalol

The PS in phase maps has been used as a valid alternative of wavebreak, which serves as a source of VF[13–15]. In the present study, therapeutic concentrations (10 mg/L) of *d,l*-sotalol significantly decreased the average number of PSs in each phase map, which indicated that *d,l*-sotalol effectively reduced wavebreak during VF. Also, administration of *d,l*-sotalol facilitated the occurrence of long-lasting reentry and increased the percentage of recording time containing organized reentry during VF, leading to a reduction in wavefront complexity. Several possible mechanisms may contribute to this anti-fibrillatory effect.

APD and WL Prolongation The WL hypothesis posits that reentry excitation is only possible if the WL of the propagating wave is shorter than the reentry path length[17,18]. As shown in this study (**Table 1**), *d,l*-sotalol progressively lengthened the APD_{70} and WL with increasing concentrations. Therefore, the same amount of cardiac tissue could support fewer reentrant circuits than at baseline, leading to reduced complexity of VF activation and the cessation of VF.

Inconsistent with this notion, APD prolongation may adversely enhance wavebreak and increase wavefront complexity. It has been reported by Yamazaki et al that nifekalant, an I_{Kr} blocker, increased the average number of PSs during spiral-type reentrant VT in 2-dimensional rabbit ventricular myocardial tissue preparations, because the wave front frequently encountered its own tail[19]. Although that phenomenon (ie, enhancement of wavebreak because of APD prolongation) was not observed in the present study using 3-dimensional tissue preparations and therapeutic concentrations (≤10 mg/L) of *d,l*-sotalol, it is possible that further lengthening of the APD with higher concentrations (>10 mg/L) of *d,l*-sotalol may facilitate wavebreak via wave front–tail interaction and thus increase the complexity of VF activation.

APD Restitution Flattening A steep APDR predisposes the spiral waves of VF to break up into multiple wavelets and facilitates the maintenance of VF[20]. By modifying the APDR characteristics, drugs that can flatten the APDR show anti-fibrillatory activity[21,22]. However, previous experimental studies provide conflicting evidence about the effects of sotalol on APDR[4,23,24] which may be related in part to the different animal species[4,24], concentrations of *d,l*-sotalol[4], isomers of sotalol (*d*-sotalol or *d,l*-sotalol)[4,24,25] and different cardiac tissues (atrium or ventricle)[4,24,26]. Pak et al have demonstrated that β-blockers significantly reduce the VF CL and flatten the APDR[12]. The β-adrenergic blocking activity of racemic sotalol is almost entirely derived from the *l*-isomer[27–30] so *d,l*-sotalol may have a greater APDR flattening effect than *d*-sotalol[4,24].

It has been reported by Pak et al that *d,l*-sotalol at therapeutic doses (≤10 mg/L) flattened the APDR in isolated swine RV tissues; however, a higher concentration (20 mg/L) adversely steepened the APDR and enhanced VF inducibility[4]. Similar to their findings, we found that that *d,l*-sotalol at 5–10 mg/L also decreased the maximum slope of APDR in isolated rabbit ventricles. APDR flattening by *d,l*-sotalol per se may decrease the break-up of spiral waves and enhance the occurrence of long-lasting organized reentry, thereby reducing the complexity of VF activation.

No Enhancement of APD Dispersion and Spatial Heterogeneity of Restitutions It is well known that *d*-sotalol increases the transmural QT dispersion, mimicking the HERG defect in long QT 2 syndrome, and predisposes the ventricular substrate to the formation of VF[31,32]. However, *d,l*-sotalol at therapeutic concentrations has not been reported to accentuate APD dispersion in either canine atria[33] or rabbit ventricles[34]. Consistent with those findings, in the present study the use of 5 or 10 mg/L *d,l*-sotalol did not increase the spatial dispersion of APD. Furthermore, the spatial heterogeneity of the APD and CT^{-1} restitutions was not enhanced by *d,l*-sotalol.

Presence of Long-Lasting Non-Stationary Reentry Before VF Termination

To the best of our knowledge, the wavefront characteristics of VF during *d,l*-sotalol infusion have not been explored using an optical mapping system. A novel finding of our study is that *d,l*-sotalol at therapeutic concentrations facilitated the occurrence of long-lasting non-stationary reentry during VF. This finding is different from that reported by Chorro et al[3] who used a similar concentration (20μmol, 6.18 mg/L) of *d,l*-sotalol and an electrode mapping system with a relatively small mapped area. In their report, *d,l*-sotalol produced no significant variation in the life span (consecutive rotations) of reentry when compared with control[3]

We have reported that both D600 and propranolol can flatten the APDR and convert a multiple-wavelet VF into a slower focal-source VF (ie, type 2 VF) in isolated rabbit hearts[6,12] During type 2 VF, the mother rotor always anchored on the PM[6,7] In the present study using the same animal model, *d,l*-sotalol also enhanced the generation of epicardial reentry during VF; however, instead of anchoring on the PM, these reentries drifted before VF termination. It has also been reported that nifekalant causes a pre-existing reentry to meander drastically[19,35] The presence of non-stationary reentry can be partly explained by the WL hypothesis[17,18] As the WL is prolonged by *d,l*-sotalol, the tip of the reentrant wavefront had to move in a much wider pattern to maintain a sufficient excitable gap, resulting in meandering. On the other hand, as the WL is shortened by D600[6] the reentry can stably anchor on the PM with an adequate excitable gap in the same amount of ventricular tissue, leading to the formation of either VT or type 2 VF.

With nifekalant infusion in a 2-dimensional layer of rabbit ventricular myocardium[19] meandering reentrant wavefronts can be extinguished by 2 mechanisms: (1) collision of the drifting reentry with an anatomical boundary, and (2) trapping of the reentry tip in a region surrounded by refractory tissue. Although we did not exactly record the activations immediately before VF termination in this study, it is possible that these mechanisms contributed to the termination of VF during *d,l*-sotalol infusion.

Study Limitations

Firstly, the 30-min washout data showed that the DF of VF was still significantly lower when compared with baseline, which suggests that a 30-min washout period may not be sufficient to completely eliminate the effect of *d,l*-sotalol from rabbit ventricular tissues. Secondly, it is unclear whether or not the findings of this study are applicable to VF in larger and/or diseased ventricles, because geometry and tissue mass influence the dynamics of spiral reentry. Functional remodeling of ion channels and calcium-handling proteins in diseased hearts may also modify the dynamics of functional reentry. Finally, this study only used therapeutic concentrations (≤10 mg/L) of *d,l*-sotalol. Higher concentrations (>10 mg/L) of *d,l*-sotalol steepen the APDR and further lengthen WL[4] Both of those effects may potentially enhance wavebreak[19,20] and subsequently increase wavefront complexity. Therefore, the effects of *d,l*-sotalol at higher concentrations (>10 mg/L) on wavefront dynamics of VF may be different from those at therapeutic concentrations and deserve further investigation.

Acknowledgments

We thank Robin Tsai and Kai-Yuan Cheng for their assistance. We also thank Dr Jiunn-Lee Lin (National Taiwan University Hospital, Taipei, Taiwan) for providing the intravenous form of d,l-sotalol for this study.

This study was supported in part by the National Science Council Grant 96-2628-B-010-035-MY2, Taipei, Taiwan, by Yen Tjing Ling Medical Foundation, by the Taichung Veterans General Hospital Grants TCVGH-963105C (Dr Wu), TCVGH-FCU 958215 (Dr Horng), Taichung, Taiwan, and by an Established Investigatorship Award (Dr Lin), American Heart Association, Dallas, TX, USA.

Disclosure

None.

References

1. Mason JW. A comparison of electrophysiologic testing with Holter monitoring to predict antiarrhythmic-drug efficacy for ventricular tachyarrhythmias: Electrophysiologic Study versus Electrocardiographic Monitoring Investigators. *N Engl J Med* 1993; **329:** 445–451.
2. Mason JW. A comparison of seven antiarrhythmic drugs in patients with ventricular tachyarrhythmias: Electrophysiologic Study versus Electrocardiographic Monitoring Investigators. *N Engl J Med* 1993; **329:** 452–458.
3. Chorro FJ, Canoves J, Guerrero J, Mainar L, Sanchis J, Such L, et al. Alteration of ventricular fibrillation by flecainide, verapamil, and sotalol: An experimental study. *Circulation* 2000; **101:** 1606–1615.
4. Pak HN, Kim YH, Hwang GS, Lee SJ, Lee HS, Lim HE, et al. Antifibrillatory and proarrhythmic effects of d,l-sotalol mediated by the action potential duration restitution kinetics. *Korean Circ J* 2005; **35:** 282–289.
5. Wu TJ, Lin SF, Weiss JN, Ting CT, Chen PS. Two types of ventricular fibrillation in isolated rabbit hearts: Importance of excitability and action potential duration restitution. *Circulation* 2002; **106:** 1859–1866.
6. Wu TJ, Lin SF, Baher A, Qu Z, Garfinkel A, Weiss JN, et al. Mother rotors and the mechanisms of D600-induced type 2 ventricular fibrillation. *Circulation* 2004; **110:** 2110–2118.
7. Pak HN, Kim GI, Lim HE, Fang YH, Choi JI, Kim JS, et al. Both Purkinje cells and left ventricular posteroseptal reentry contribute to the maintenance of ventricular fibrillation in open-chest dogs and swine. *Circ J* 2008; **72:** 1185–1192.
8. Wu TJ, Lin SF, Hsieh YC, Ting CT, Chen PS. Ventricular fibrillation during no-flow global ischemia in isolated rabbit hearts. *J Cardiovasc Electrophysiol* 2006; **17:** 1112–1120.
9. Wu TJ, Lin SF, Hsieh YC, Chen PS, Ting CT. Early recurrence of ventricular fibrillation after successful defibrillation during prolonged global ischemia in isolated rabbit hearts. *J Cardiovasc Electrophysiol* 2008; **19:** 203–210.
10. Gray RA, Pertsov AM, Jalife J. Spatial and temporal organization during cardiac fibrillation. *Nature* 1998; **392:** 75–78.
11. Valderrabano M, Lee MH, Ohara T, Lai AC, Fishbein MC, Lin SF, et al. Dynamics of intramural and transmural reentry during ventricular fibrillation in isolated swine ventricles. *Circ Res* 2001; **88:** 839–848.
12. Pak HN, Oh YS, Liu YB, Wu TJ, Karagueuzian HS, Lin SF, et al. Catheter ablation of ventricular fibrillation in rabbit ventricles treated with beta-blockers. *Circulation* 2003; **108:** 3149–3156.
13. Liu YB, Peter A, Lamp ST, Weiss JN, Chen PS, Lin SF. Spatiotemporal correlation between phase singularities and wavebreaks during ventricular fibrillation. *J Cardiovasc Electrophysiol* 2003; **14:** 1103–1109.
14. Hayashi H, Lin SF, Chen PS. Preshock phase singularity and the outcome of ventricular defibrillation. *Heart Rhythm* 2007; **4:** 927–934.
15. Valderrabano M, Chen PS, Lin SF. Spatial distribution of phase singularities in ventricular fibrillation. *Circulation* 2003; **108:** 354–359.
16. Tang L, Hwang GS, Hayashi H, Song J, Ogawa M, Kobayashi K, et al. Intracellular calcium dynamics at the core of endocardial stationary spiral waves in Langendorff-perfused rabbit hearts. *Am J Physiol Heart Circ Physiol* 2008; **295:** H297–H304.
17. Mines GR. On dynamic equilibrium in the heart. *J Physiol* 1913; **46:** 349–383.
18. Rensma PL, Allessie MA, Lammers WJ, Bonke FI, Schalij MJ. Length of excitation wave and susceptibility to reentrant atrial arrhythmias in normal conscious dogs. *Circ Res* 1988; **62:** 395–410.
19. Yamazaki M, Honjo H, Nakagawa H, Ishiguro YS, Okuno Y, Amino M, et al. Mechanisms of destabilization and early termination of spiral wave reentry in the ventricle by a class III antiarrhythmic agent, nifekalant. *Am J Physiol Heart Circ Physiol* 2007; **292:** H539–H548.

20. Weiss JN, Garfinkel A, Karagueuzian HS, Qu Z, Chen PS. Chaos and the transition to ventricular fibrillation: A new approach to antiarrhythmic drug evaluation. *Circulation* 1999; **99:** 2819–2826.
21. Garfinkel A, Kim YH, Voroshilovsky O, Qu Z, Kil JR, Lee MH, et al. Preventing ventricular fibrillation by flattening cardiac restitution. *Proc Natl Acad Sci USA* 2000; **97:** 6061–6066.
22. Riccio ML, Koller ML, Gilmour RF Jr. Electrical restitution and spatiotemporal organization during ventricular fibrillation. *Circ Res* 1999; **84:** 955–963.
23. Qu Z, Weiss JN. Effects of Na(+) and K(+) channel blockade on vulnerability to and termination of fibrillation in simulated normal cardiac tissue. *Am J Physiol Heart Circ Physiol* 2005; **289:** H1692–H1701.
24. Fei H, Frame LH. d-Sotalol terminates reentry by two mechanisms with different dependence on the duration of the excitable gap. *J Pharmacol Exp Ther* 1996; **277:** 174–185.
25. Reiter MJ, Zetelaki Z, Kirchhof CJ, Boersma L, Allessie MA. Interaction of acute ventricular dilatation and d-sotalol during sustained reentrant ventricular tachycardia around a fixed obstacle. *Circulation* 1994; **89:** 423–431.
26. Boyden PA, Graziano JN. Activation mapping of reentry around an anatomical barrier in the canine atrium: Observations during the action of the class III agent, d-sotalol. *J Cardiovasc Electrophysiol* 1993; **4:** 266–279.
27. Singh BN. Historical development of the concept of controlling cardiac arrhythmias by lengthening repolarization: Particular reference to sotalol. *Am J Cardiol* 1990; **65:** 3A–11A.
28. Singh BN. Electrophysiologic basis for the antiarrhythmic actions of sotalol and comparison with other agents. *Am J Cardiol* 1993; **72:** 8A–18A.
29. Kato R, Ikeda N, Yabek SM, Kannan R, Singh BN. Electrophysiologic effects of the levo- and dextrorotatory isomers of sotalol in isolated cardiac muscle and their in vivo pharmacokinetics. *J Am Coll Cardiol* 1986; **7:** 116–125.
30. Ishizaka T, Takahara A, Iwasaki H, Mitsumori Y, Kise H, Nakamura Y, et al. Comparison of electropharmacological effects of bepridil and sotalol in halothane-anesthetized dogs. *Circ J* 2008; **72:** 1003–1011.
31. Shimizu W, Antzelevitch C. Effects of a K(+) channel opener to reduce transmural dispersion of repolarization and prevent torsades de pointes in LQT1, LQT2, and LQT3 models of the long-QT syndrome. *Circulation* 2000; **102:** 706–712.
32. Benson AP, Aslanidi OV, Zhang H, Holden AV. The canine virtual ventricular wall: A platform for dissecting pharmacological effects on propagation and arrhythmogenesis. *Prog Biophys Mol Biol* 2008; **96:** 187–208.
33. Nattel S, Bourne G, Talajic M. Insights into mechanisms of antiarrhythmic drug action from experimental models of atrial fibrillation. *J Cardiovasc Electrophysiol* 1997; **8:** 469–480.
34. Kirchhof P, Milberg P, Eckardt L, Breithardt G, Haverkamp W. Effect of sotalol and acute ventricular dilatation on action potential duration and dispersion of repolarization after defibrillation shocks. *J Cardiovasc Pharmacol* 2003; **41:** 640–648.
35. Kodama I, Honjo H, Yamazaki M, Nakagawa H, Ishiguro Y, Okuno Y, et al. Optical imaging of spiral waves: Pharmacological modification of spiral-type excitations in a 2-dimensional layer of ventricular myocardium. *J Electrocardiol* 2005; **38:** 126–130.